

Supporting Information

New Journal of Chemistry

Molecular Engineering of Fluorescent Bichromophore 1,3,5-Triaryl- Δ^2 -Pyrazoline and 4-Amino-1,8- Naphthalimide Molecular Logic Gates

Darlene Sammut,^a Nathalie Bugeja,^a Konrad Szaciłowski^b and
David C. Magri^a

^a Department of Chemistry, Faculty of Science, University of Malta, Msida, MSD 2080, Malta. E-mail: david.magri@um.edu.mt

^b AGH University of Science and Technology, Academic Centre for Materials and Nanotechnology, Mickiewicza 30, 30-059 Kraków, Poland. Email: szacilow@agh.edu.pl

Table of Contents

| | |
|--|-------|
| Chemicals | 2 |
| Instrumentation | 2 |
| Titration Procedure | 3 |
| Fluorescence Quantum Yields | 3 |
| Fig. S1-S3 ¹ H NMR spectra of 1-3 in CDCl ₃ with 0.03% TMS..... | 4-6 |
| Fig. S4-S6 ¹³ C NMR spectra of 1-3 in CDCl ₃ with 0.03% TMS..... | 7-9 |
| Fig. S7-S9 IR spectra of 1-3 using KBr disc method. | 10-12 |
| Fig. S10-12 HRMS of 1-3 by ESI-TOF..... | 13-15 |
| Fig. S13 Molecule 1 in different solvents irradiated with a 365 nm UV-lamp..... | 16 |
| Fig. S14 Molecule 2 in various solvents under a 365 nm UV-lamp..... | 16 |
| Fig. S15 UV-Vis absorption spectra of 1 at 10 ⁻⁶ M..... | 17 |
| Fig. S16 Fluorescence emission spectra of 1 at 10 ⁻⁶ M..... | 17 |
| Fig. S17 UV-Vis absorption spectra of 2 at 10 ⁻⁶ M..... | 18 |
| Fig. S18 Fluorescence emission spectra of 2 at 10 ⁻⁶ M..... | 18 |
| Fig. S19 Solid samples of 1 and 2 irradiated with a 365 nm UV-lamp..... | 19 |
| Fig. S20 Titration curves and linearized Henderson-Hasselbalch plots of 1 and 2 | 20 |
| Fig. S21 Titration curves and linearized Henderson-Hasselbalch plots of 3 | 21 |
| Fig. S22 Energy level HOMO-LUMO diagrams for 1-3 | 22 |
| Table S1 Summary of the photophysical properties of 1 in various solvents..... | 23 |
| Table S2 Summary of the photophysical properties of 2 in various solvents..... | 24 |
| Table S3 Frontier orbitals calculated for molecules 1-3 and their corresponding protonated and oxidized forms at the B3LYP/6-31+g(d,p) level of theory..... | 25 |
| Table S4 Energies (in eV) of electronic levels of 1-3 and their charged derivatives calculated at B3LYP/6-31+g (d,p) theory level in THF..... | 26 |

Chemicals

4-Chloro-1,8-naphthalic anhydride (94%, Alfa Aesar, GPR), methylamine solution, 2M in THF (Argos Organics, GPR), 1,4-dioxane (Fischer Scientific, GPR), glacial acetic acid (Scharlau, ACS), 2-methoxyethanol (Carlo Erba, RPE), hydrazine monohydrate (64-65%, Sigma Aldrich, GPR), tetrahydrofuran (Carlo Erba, analytical grade), hydrochloric acid (37%, Carlo Erba, analysis grade), ethanol (96%, Carlo Erba, ACS), acetophenone (>99%, Fluka, analytical reagent grade), benzaldehyde, *N,N*-dimethylanilinebenzaldehyde (Carlo Erba, ACS), ferrocenecarboxyaldehyde (97%, BDH, GPR), chloroform-*d* with 0.03% tetramethylsilane (99.8%, Aldrich, NMR), ferric perchlorate hydrate (Sigma Aldrich, GPR), methanesulfonic acid (99%, Sigma Aldrich, GPR), sodium hydroxide (Fischer, analytical grade). All reagents and solvents were used as received. Thin-layer chromatography was performed on pre-coated silica gel plates on aluminium foils (Sigma-Aldrich, 0.2 mm, 20 × 20 cm, F₂₅) developed in a closed chamber and irradiated with 254 nm or 365 nm UV light.

Instrumentation

Syntheses were performed in round-bottom flasks immersed in a mineral oil bath heated with IKA C-MAG HS 7 hotplates fitted with an IKA ETS-D5 temperature probe. Melting points were recorded on a Stuart SMP11 (digital) melting point apparatus in open-end capillary tubes and were corrected by calibration with pure caffeine (m.p. = 235 °C). ¹H and ¹³C NMR spectra were recorded on Bruker Avance III Ascend 500 HD NMR spectrometer equipped with a 11.75 Tesla superconducting magnet and a 5 mm multinuclear PABBO probe operating at 500.13 MHz (¹H NMR) and 125.76 MHz (¹³C NMR). NMR samples were typically of 5 mg or greater dissolved in 0.8 mL of deuterated CDCl₃. was used as the internal reference standard. Chemical shifts are reported in ppm downfield from tetramethylsilane (TMS) at 0.00 ppm. All spectra were carried out at 298 K. The data was processed using Topspin Software version 3.2. Infrared spectra were recorded using Shimadzu IRAffinity-1 spectrophotometer with spectra recorded in wavenumbers (cm⁻¹). The Infrared spectrophotometer was calibrated against a blank measurement salt plate prior to adding the sample. Samples were prepared using KBr disc method. HRMS was performed by ES-ToF technique and performed by Medac Ltd (UK).

UV-vis absorption spectra were recorded at room temperature on a Jasco V-650 spectrophotometer using quartz Suprasil cells with a path length of 1.0 cm. The settings were set at 2.0 nm bandwidth with a medium response and scan speed of 400 nm min⁻¹. All spectra

were corrected by scanning the solvent as the blank solution prior to measurement of spectra. Samples were typically scanned over the range of 350-700 nm.

Fluorescence measurements were recorded at room temperature on Jasco FP-8300 spectrophotometer using Suprasil quartz cells with a path length of 1.0 cm. The parameters were set to emission mode using an excitation wavelength of 440 nm for all three molecules. The emission range was 450-700 nm region. The parameters were set at an excitation bandwidth of 1.0 nm, emission bandwidth of 2.5 nm, 50 m sec response, medium sensitivity, and a scan speed of 200 nm min⁻¹. The prepared solutions had absorbance values below 0.1 All spectra were corrected by scanning the solvent as the blank solution prior to measurement of spectra.

Titration Procedure

Standard stock solutions of **1-3** were prepared by adding 5 mg of each sample in a 100 mL volumetric flask (grade B) and made up to the mark with THF. The maximum wavelength and absorbance of each solution was determined using UV-vis spectra, and solutions diluted until the absorbance was approximately 0.1 with concentrations ca. 10 μM for **1** and **2**, and 20 μM for **3** in 50 mL grade B volumetric flasks. Molar equivalents of 1 M HCl and 0.01 M iron (III) solution were added separately into vials using Gibson 1-10 μL and 50-200 μL pipettes and eppendorf pipette tips, and transferred to a 1.0 cm Suprasil quartz cuvette. A blank measurement was run using THF and the fluorescence of each solution on addition of aliquots of acid and iron (III) solutions were measured. The excitation wavelength was 440 nm.

Fluorescence Quantum Yields

UV-vis absorption spectra of **1-3** were measured by dissolving 5 mg of sample in 100 mL of solvent and diluting to an absorbance of 0.1. Fluorescence quantum yield were calculated using the equation below:

$$\Phi_F = \frac{Area_{sample}}{Area_{standard}} \times \frac{Abs_{standard}}{Abs_{sample}} \times \frac{n_{sample}^2}{n_{standard}^2} \times \Phi_{standard}$$

where the $\Phi_{standard}$ is the fluorescence quantum yield of quinine sulfate in 0.1 M aerated aqueous sulfuric acid ($\Phi_F = 0.55$) or fluorescein in aerated aqueous water with 0.1 M NaOH ($\Phi_F = 0.95$). Calculations used the area under the emission curve of the sample and standard, the λ_{max} , absorbance of the sample and standard, and the refractive indexes of the various solvents given in Table S1 and S2.

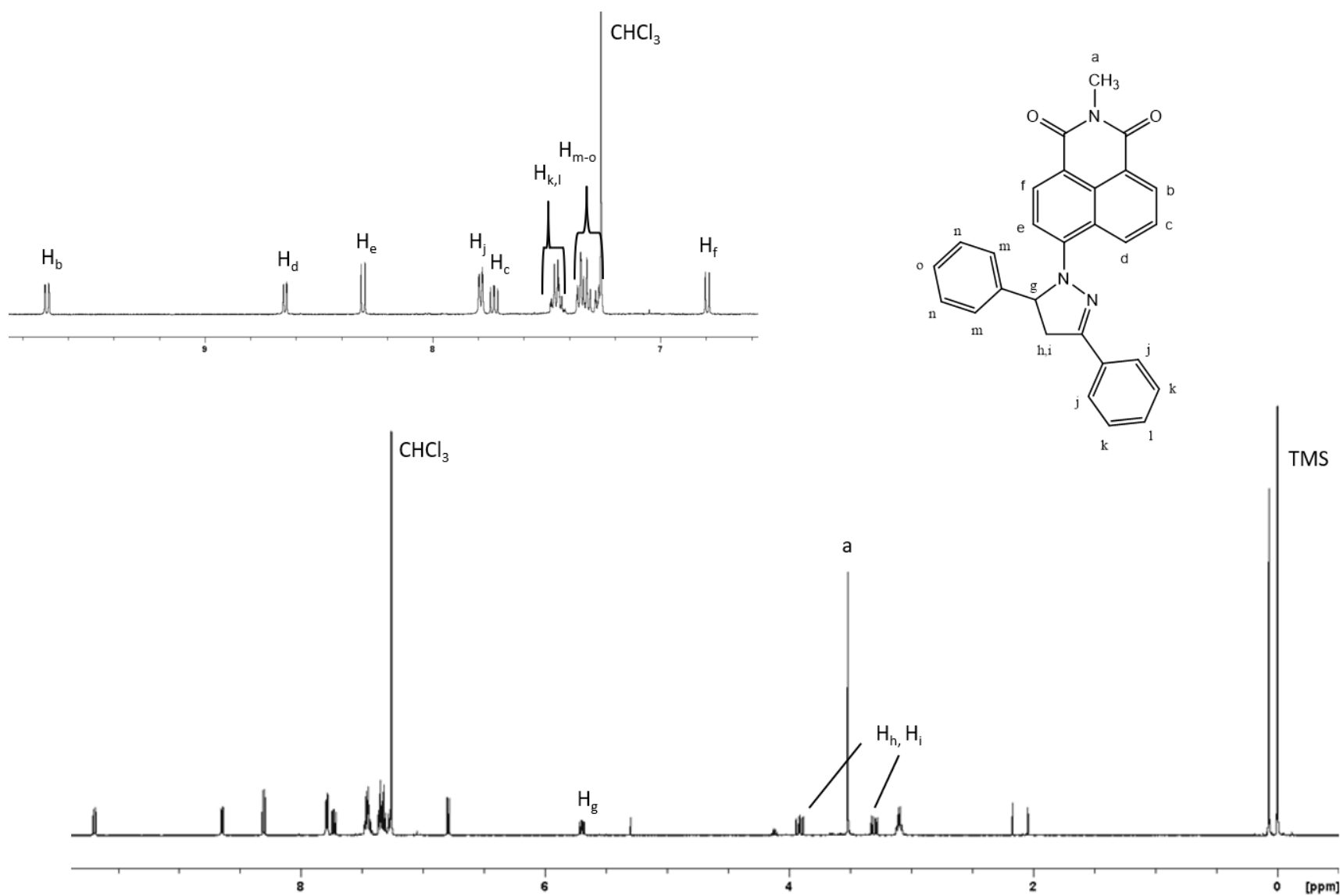


Fig. S1 ^1H NMR spectrum of **1** in CDCl_3 with 0.03% TMS.

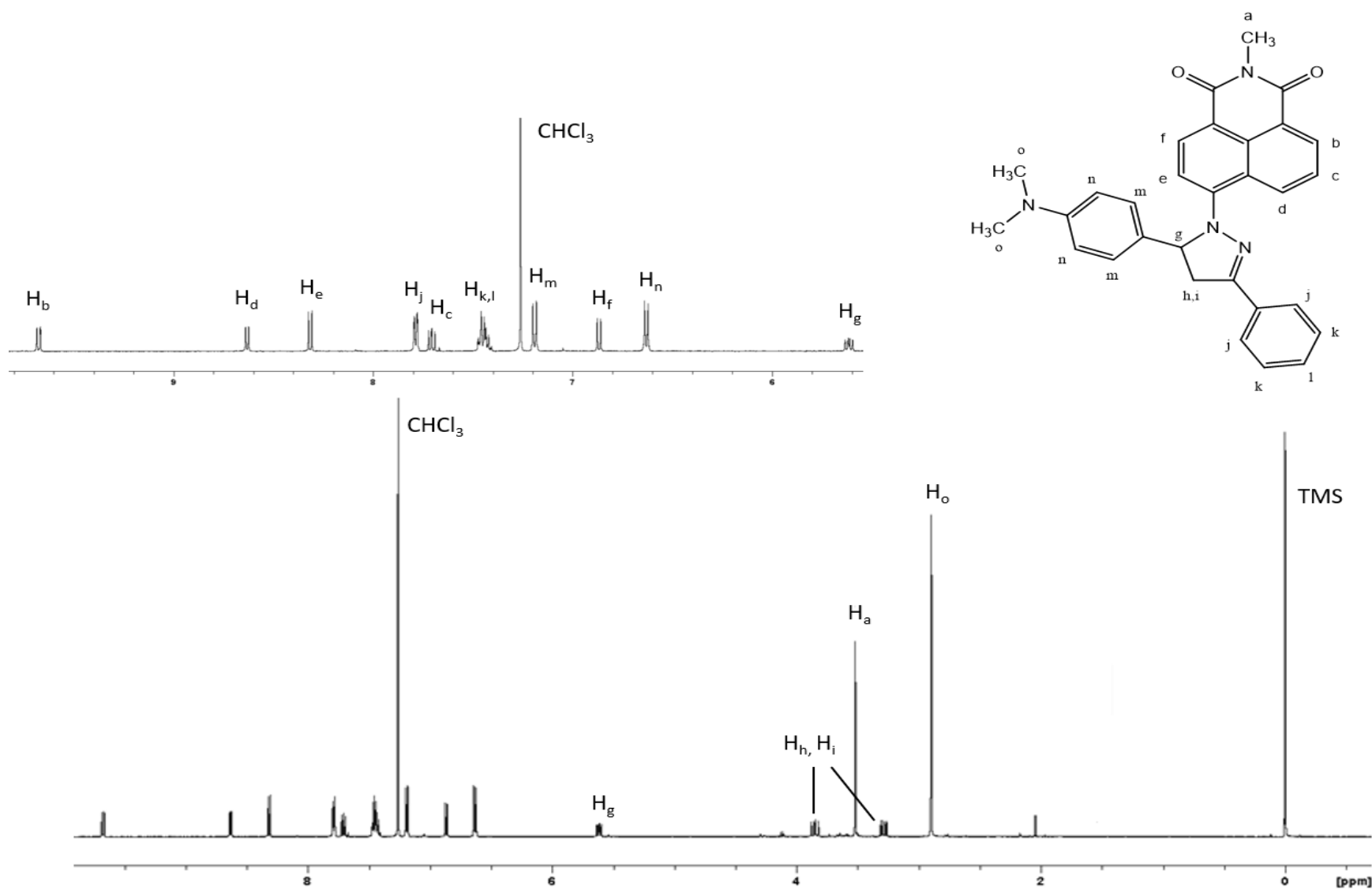


Fig. S2 ^1H NMR spectrum of **2** in CDCl_3 with 0.03% TMS.

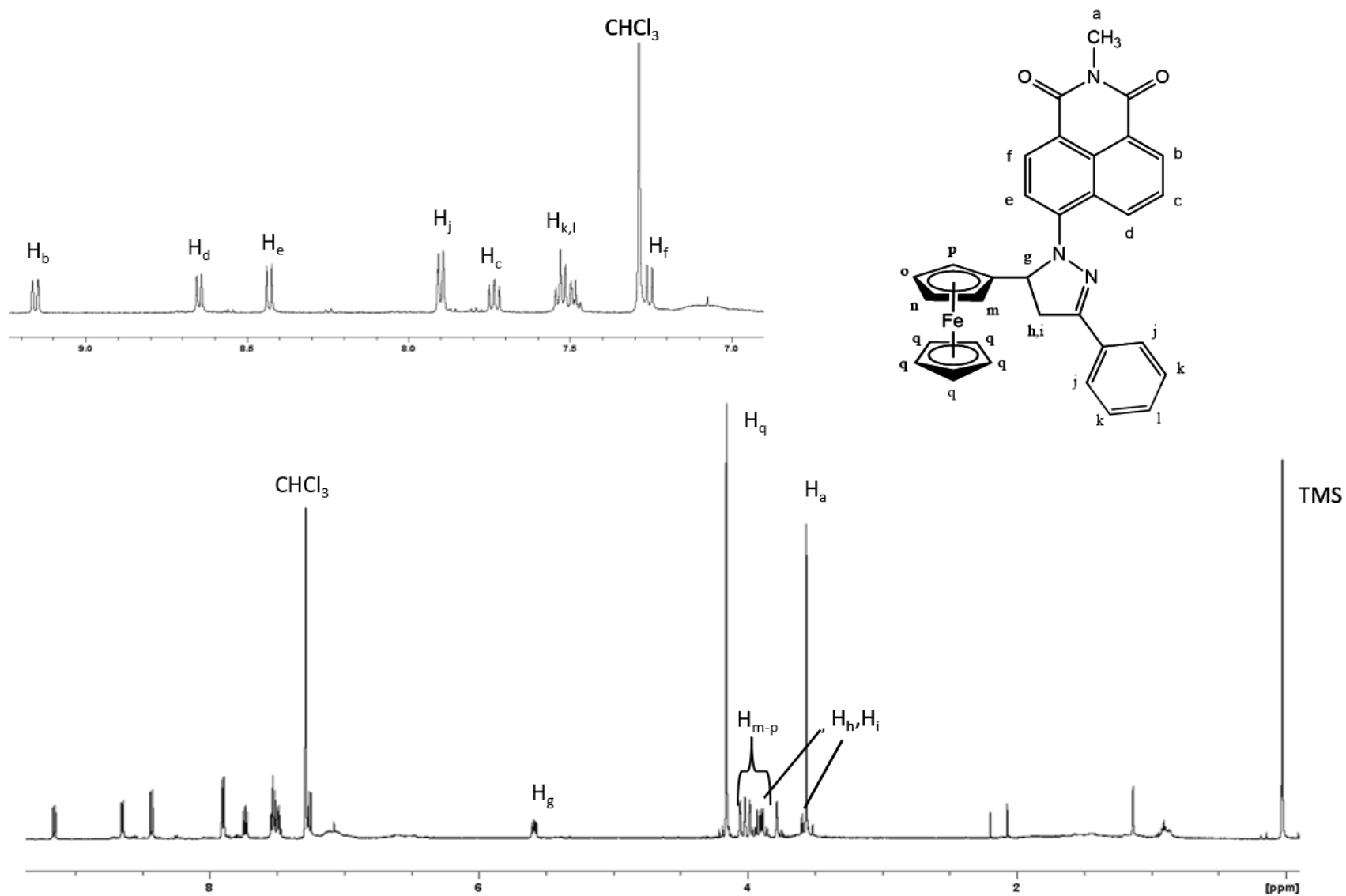


Fig. S3 ^1H NMR spectrum of **3** in CDCl_3 with 0.03% TMS.

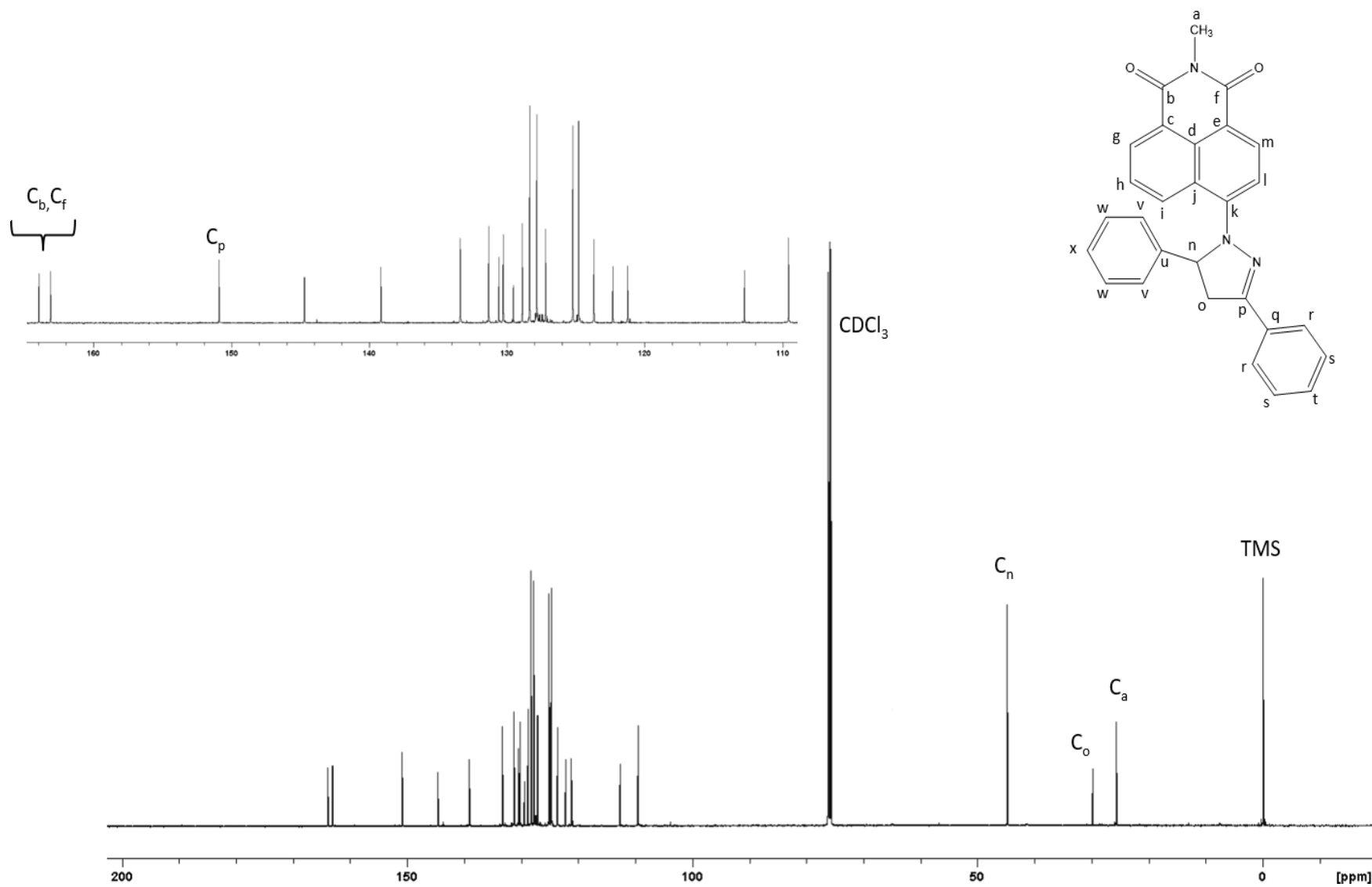


Fig. S4 ^{13}C NMR spectrum of **1** in CDCl_3 with 0.03% TMS.

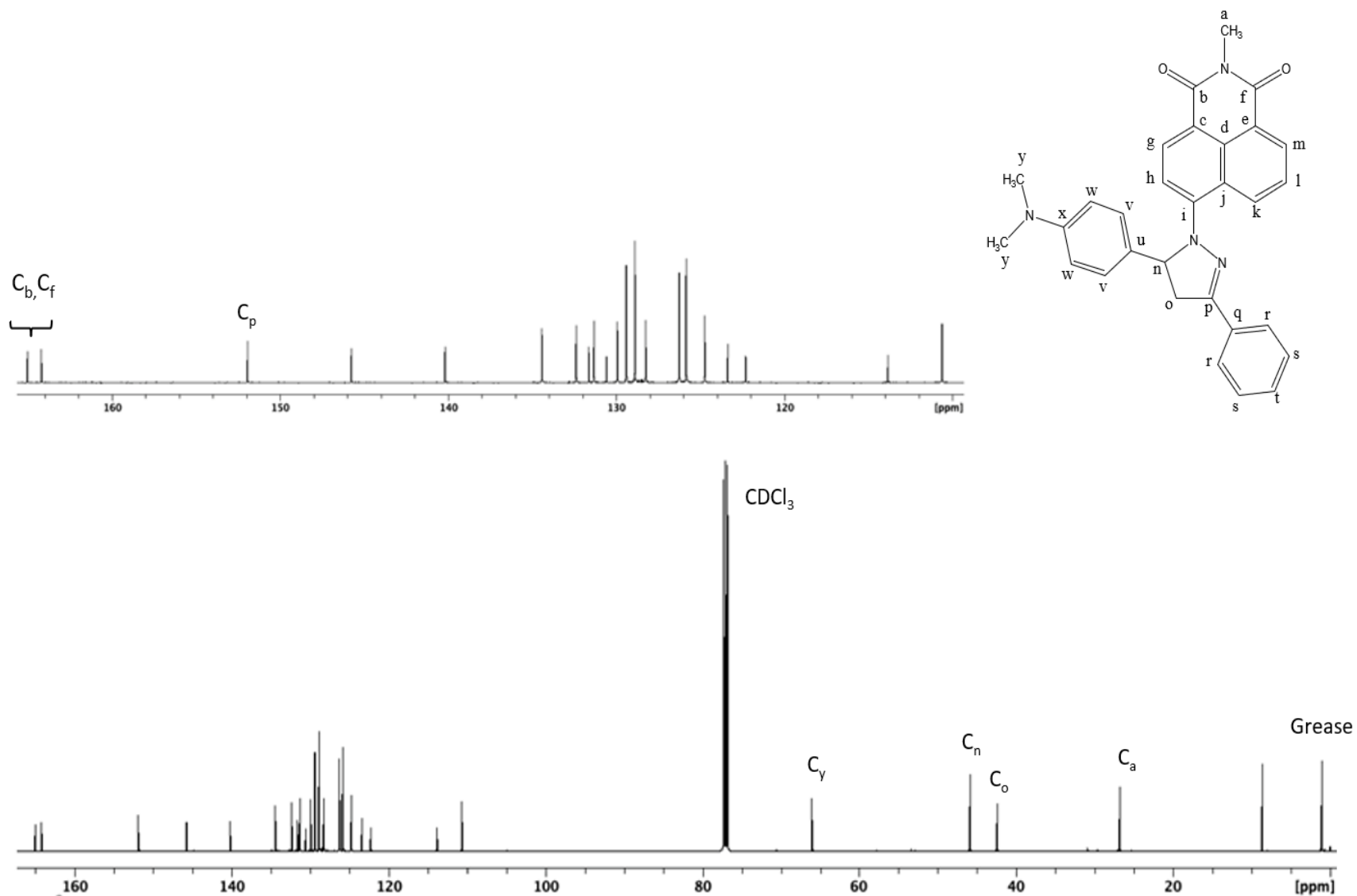


Fig. S5 ^{13}C NMR spectrum of **2** in CDCl_3 with 0.03% TMS.

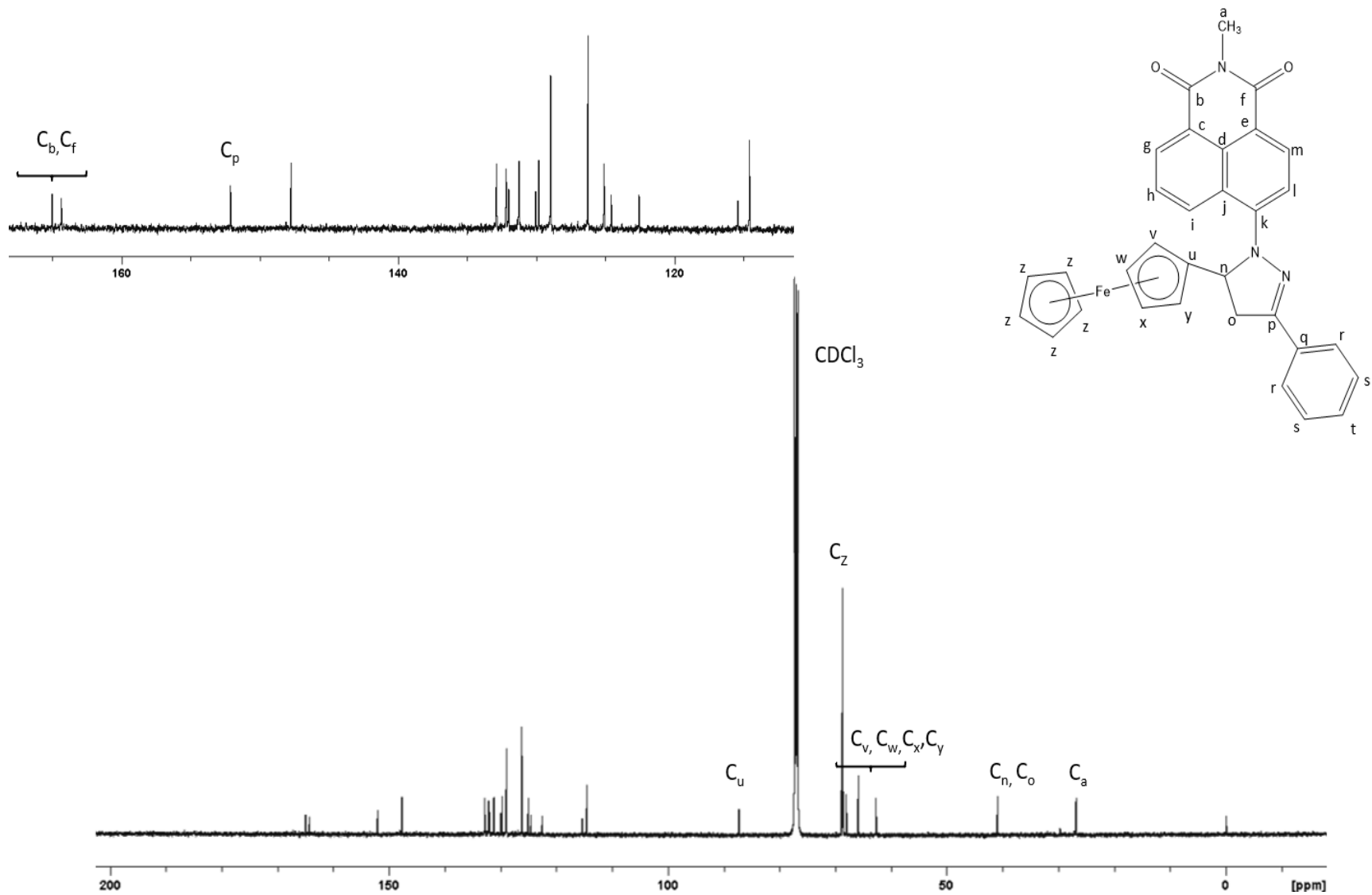


Fig. S6 ^{13}C NMR spectrum of **3** in CDCl_3 with 0.03% TMS.

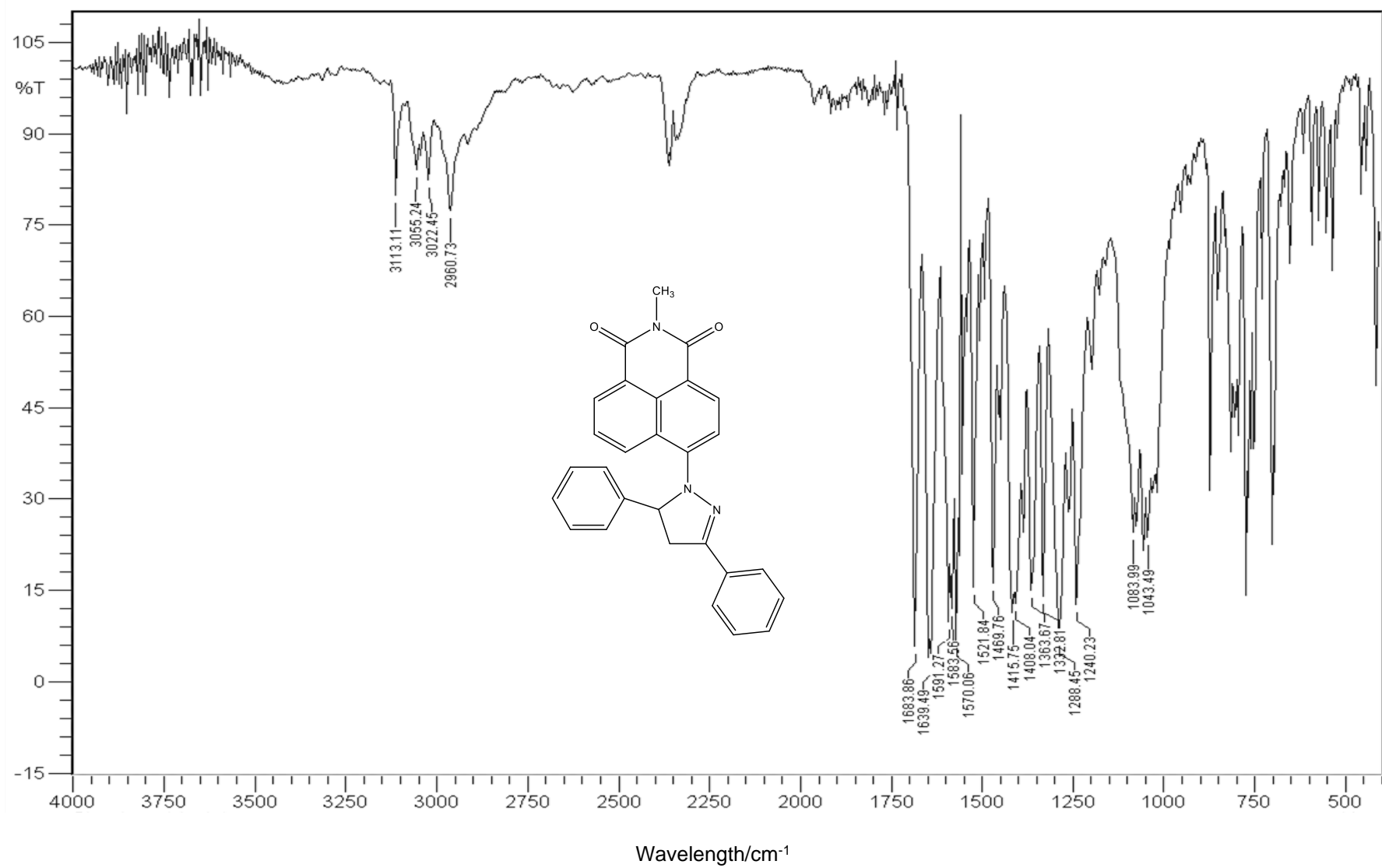


Fig S7 IR spectrum of **1** using KBr disc method.

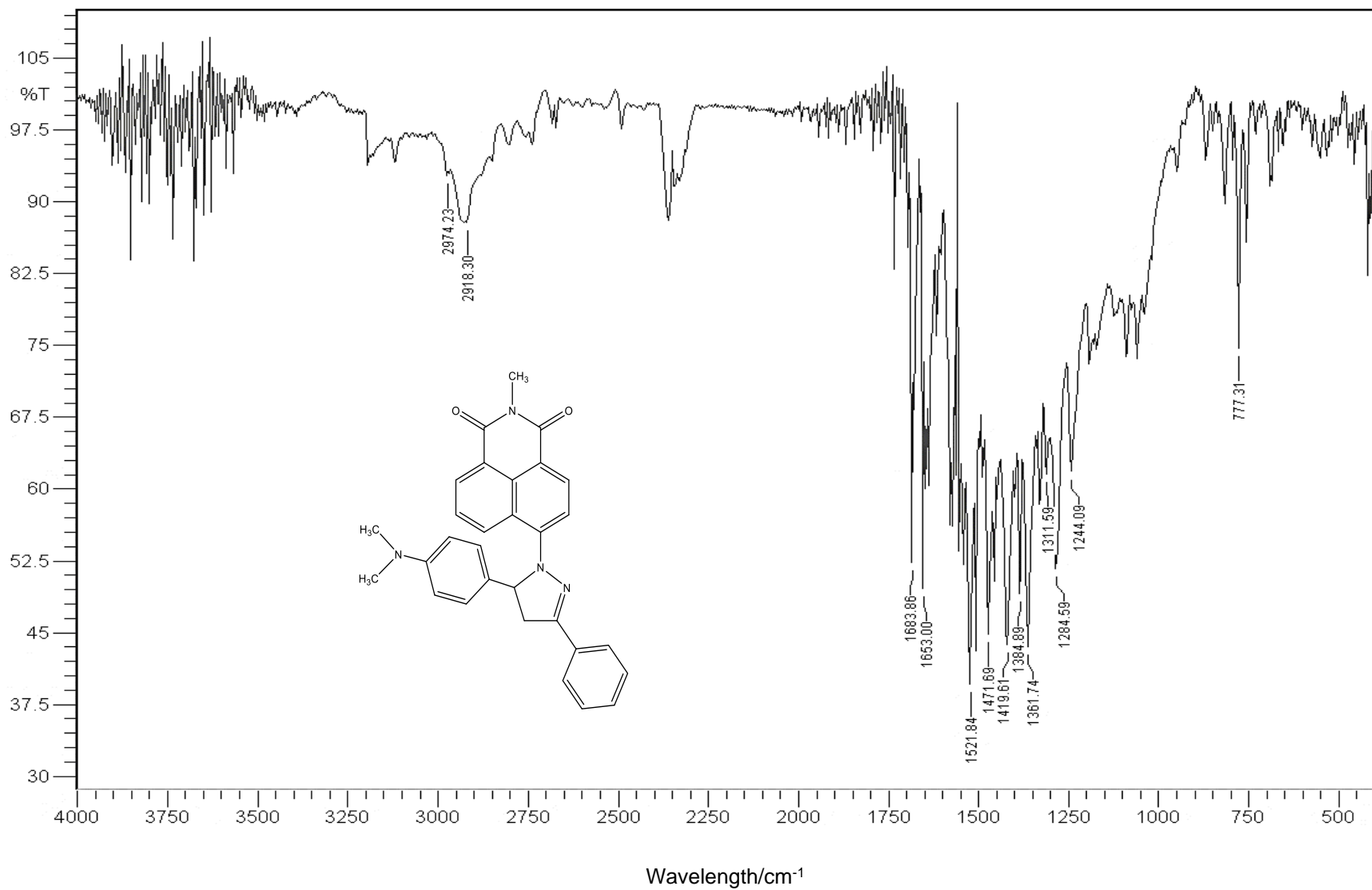


Fig. S8 IR spectrum of **2** using KBr disc method.

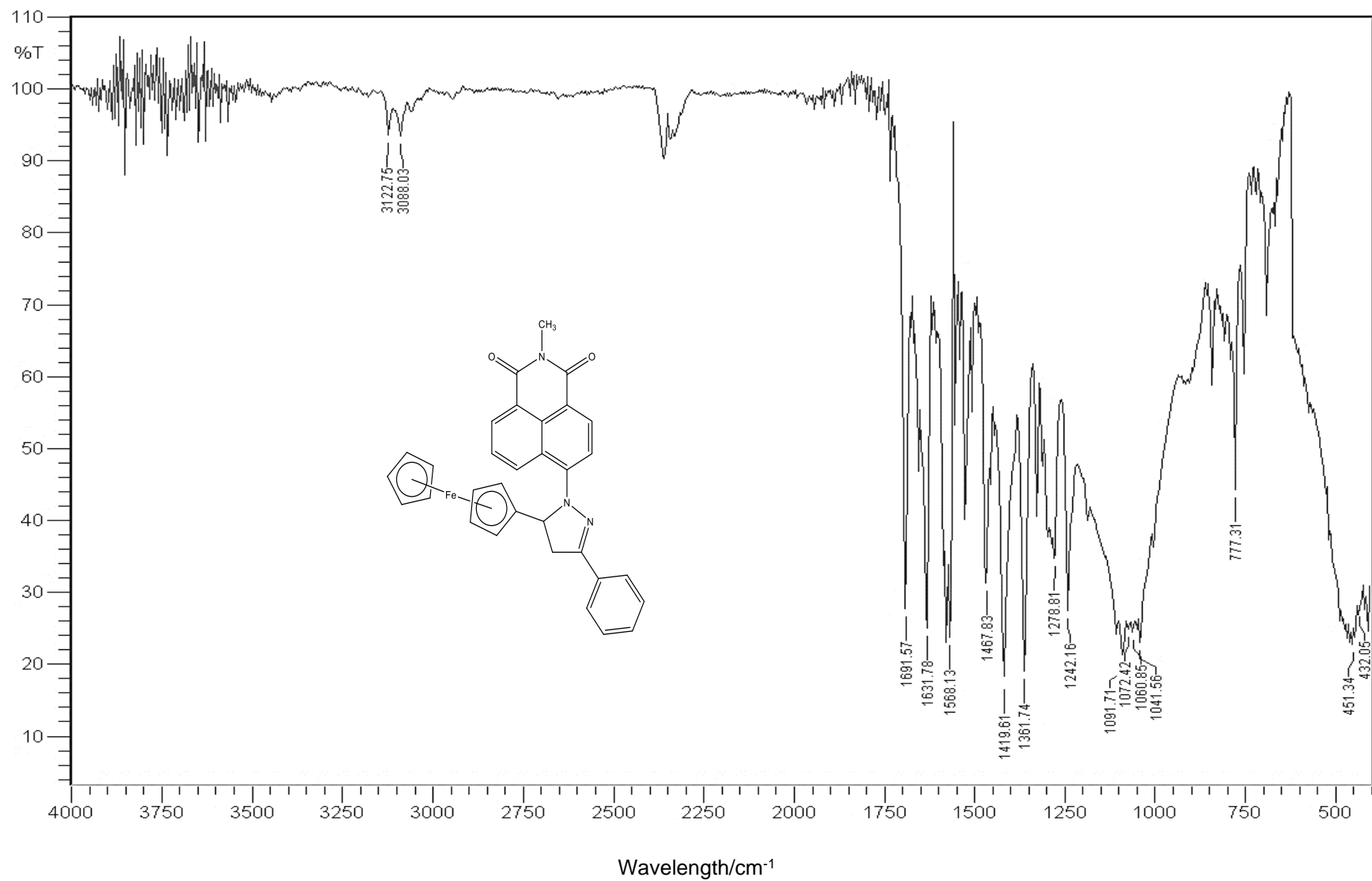


Fig. S9 IR spectrum of **3** using KBr disc method.

MEDAC_DS1
MEDAC_DS1A 8 (0.255)

19-Jul-2019
1: TOF MS ES+
259

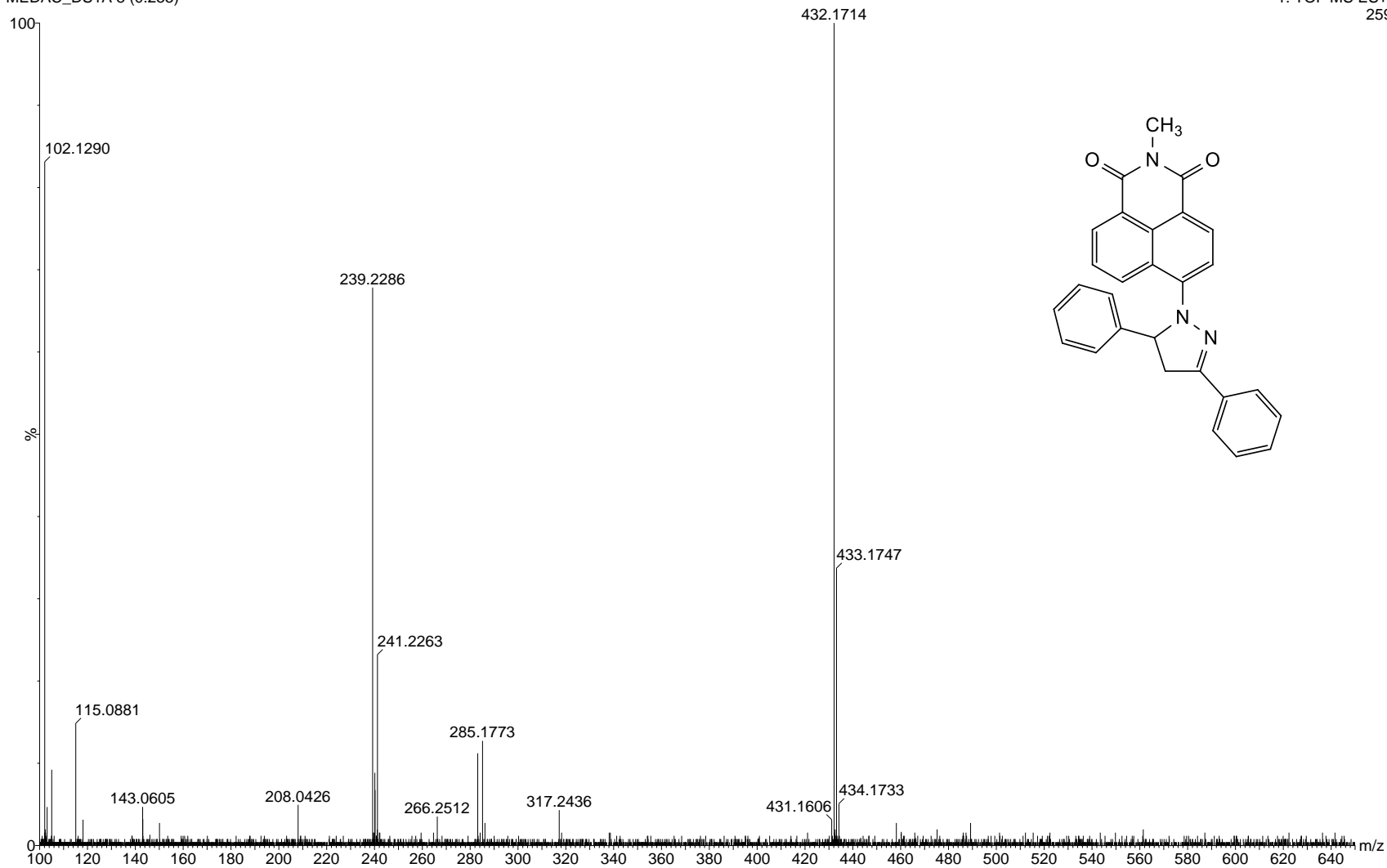


Fig. S10 HRMS of **1** by ESI-TOF.

| Mass | Calc. Mass | mDa | PPM | DBE | i-FIT | Formula |
|----------|------------|-----|-----|------|-------|---|
| 432.1714 | 432.1712 | 0.2 | 0.5 | 19.5 | 48.9 | C ₂₈ H ₂₂ N ₃ O ₂ |

MEDAC_DS2
MEDAC_DS2 8 (0.254)

19-Jul-2019
1: TOF MS ES+
1.01e3

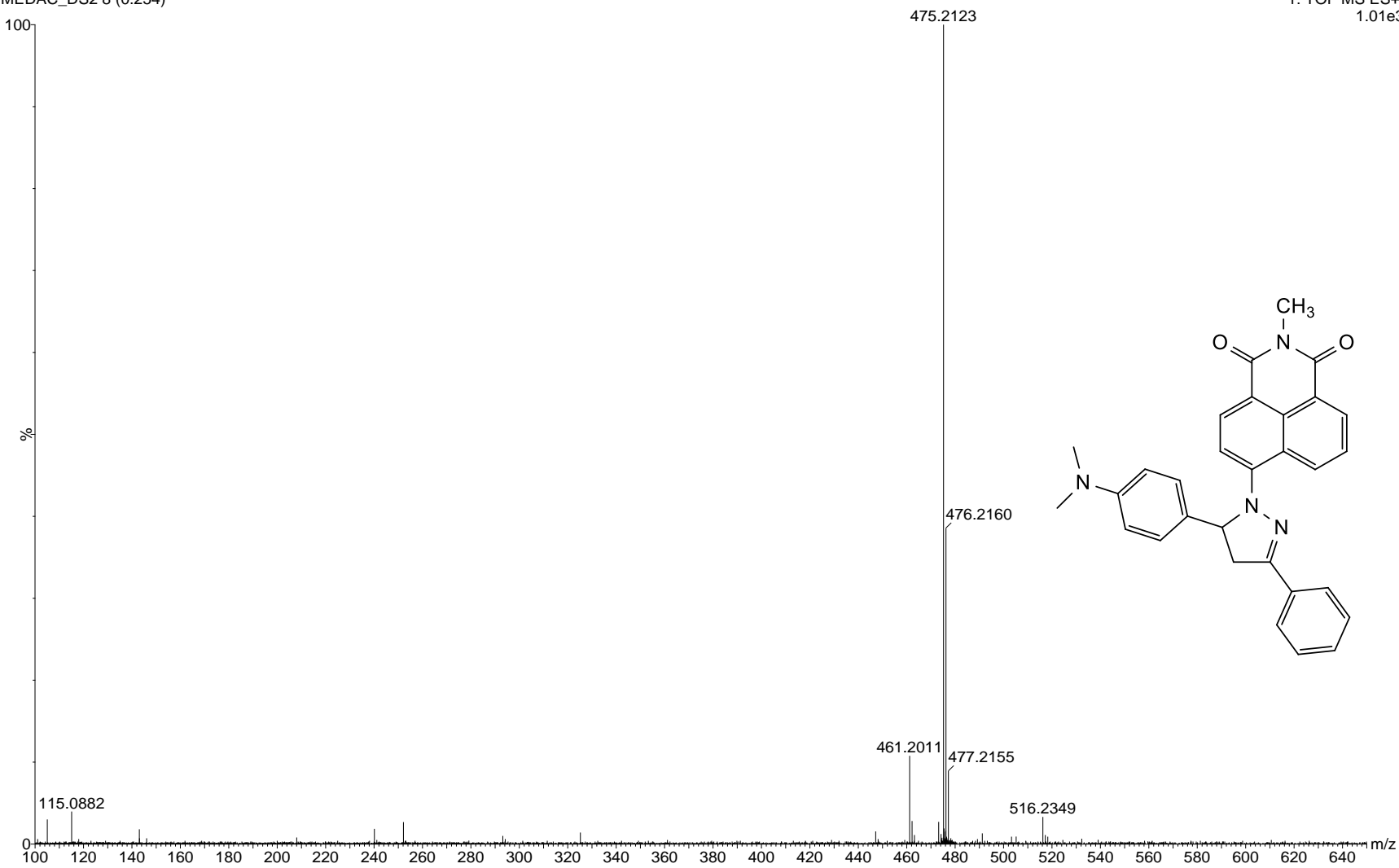


Fig. S11 HRMS of **2** by ESI-TOF.

| Mass | Calc. Mass | mDa | PPM | DBE | i-FIT | Formula |
|----------|------------|------|------|------|-------|------------|
| 475.2123 | 475.2134 | -1.1 | -2.3 | 19.5 | 96.6 | C30H27N4O2 |

180820_NB53 #85 RT: 0.39 AV: 1 NL: 6.17E9
T: FTMS + p APCI corona Full ms [125.0000-800.0000]

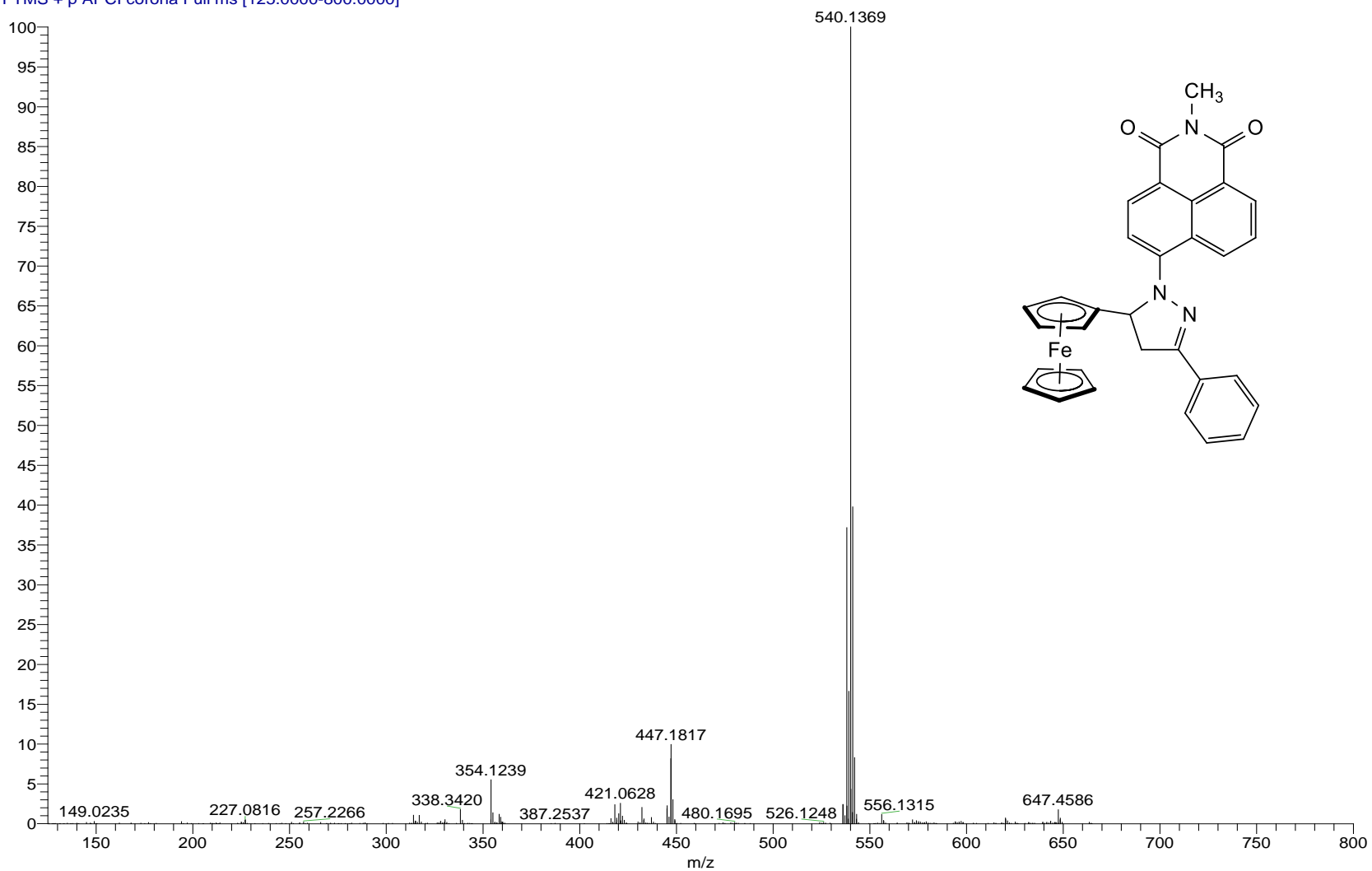


Fig. S12 HRMS of **3** by ESI-TOF.

| Mass | Calc. Mass | mDa | PPM | DBE | i-FIT | Formula |
|----------|------------|------|-------|------|-------|--|
| 540.1369 | 540.1374 | -0.5 | 0.008 | 21.5 | - | C ₃₂ H ₂₆ N ₃ O ₂ Fe |



Fig. S13 Molecule **1** at 10^{-6} M in different solvents irradiated with a 365 nm UV-lamp. From left to right: hexane, carbon tetrachloride, benzene, chloroform, octan-1-ol and pyridine.

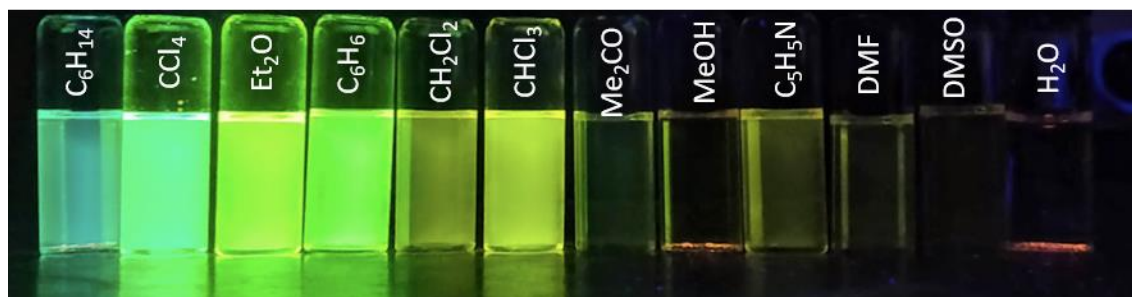


Fig. S14 Molecule **2** at 10^{-6} M in various solvents under a 365 nm UV-lamp. From left to right: hexane, carbon tetrachloride, diethyl ether, benzene, dichloromethane, chloroform, acetone, methanol, pyridine, *N,N*-dimethylformamide, dimethylsulfoxide and water. Note undissolved solid in methanol and water.

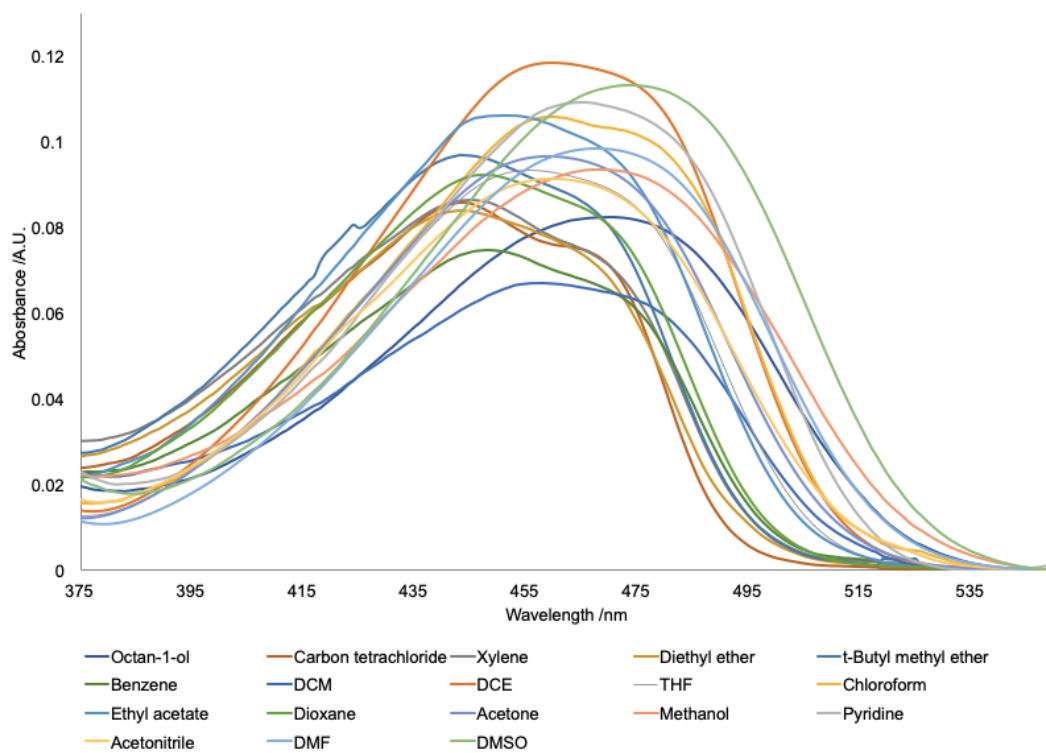


Fig. S15 UV-Vis absorption spectra of **1** at 10^{-6} M.

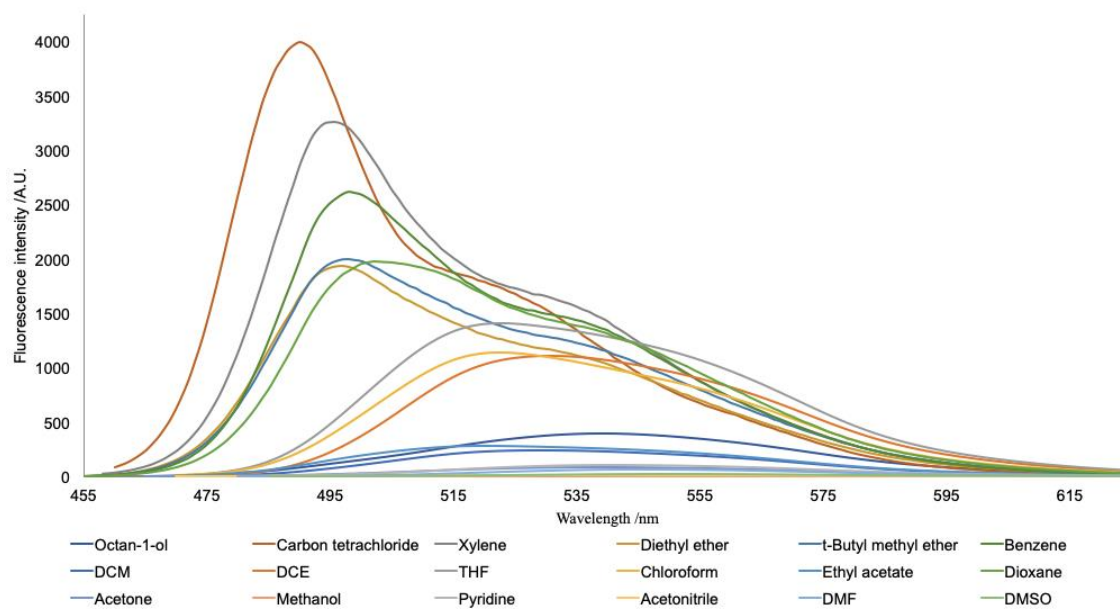


Fig. S16 Fluorescence emission spectra of **1** at 10^{-6} M excited at each respective λ_{max} .

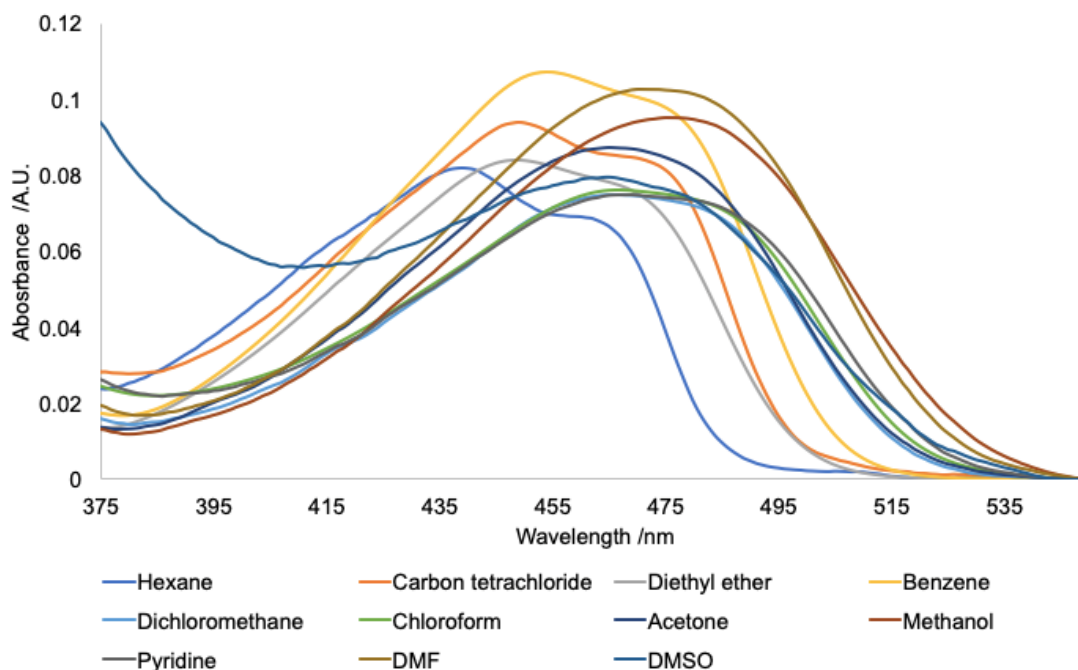


Fig. S17 UV-Vis absorption spectra of **2** at 10^{-6} M.

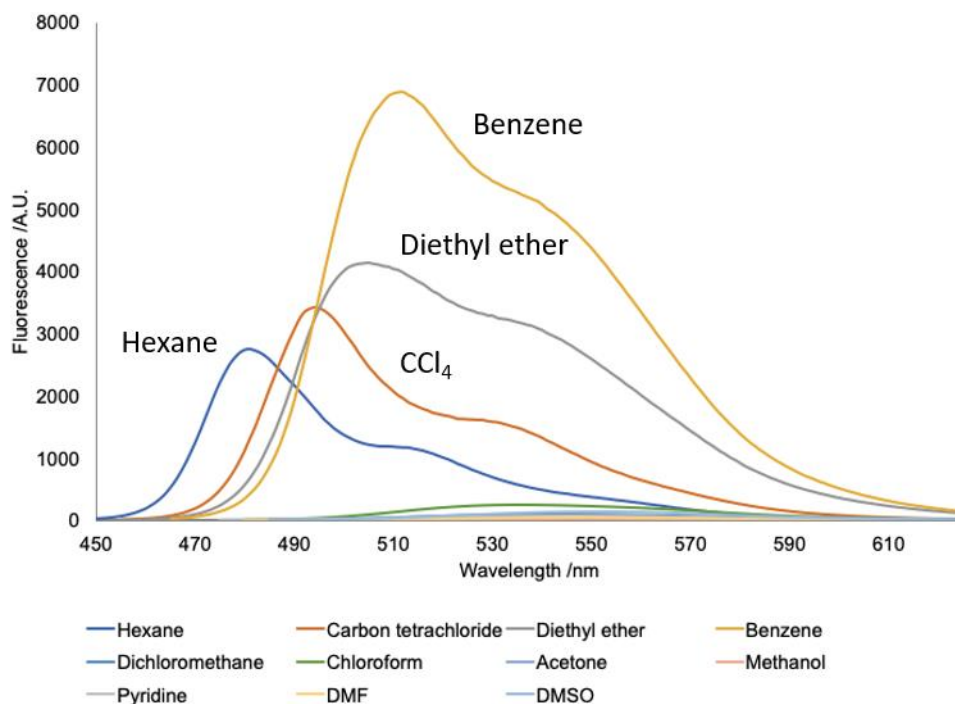


Fig. S18 Emission spectra of **2** at 10^{-6} M. Each solution was excited at its respective λ_{\max} . Solutions of **2** in acetone, methanol, pyridine, DMF and DMSO are non-fluorescent. Solution concentrations varied.



Fig. S19 Solid samples of **1** (left) and **2** (right) irradiated with a 365 nm UV lamp.

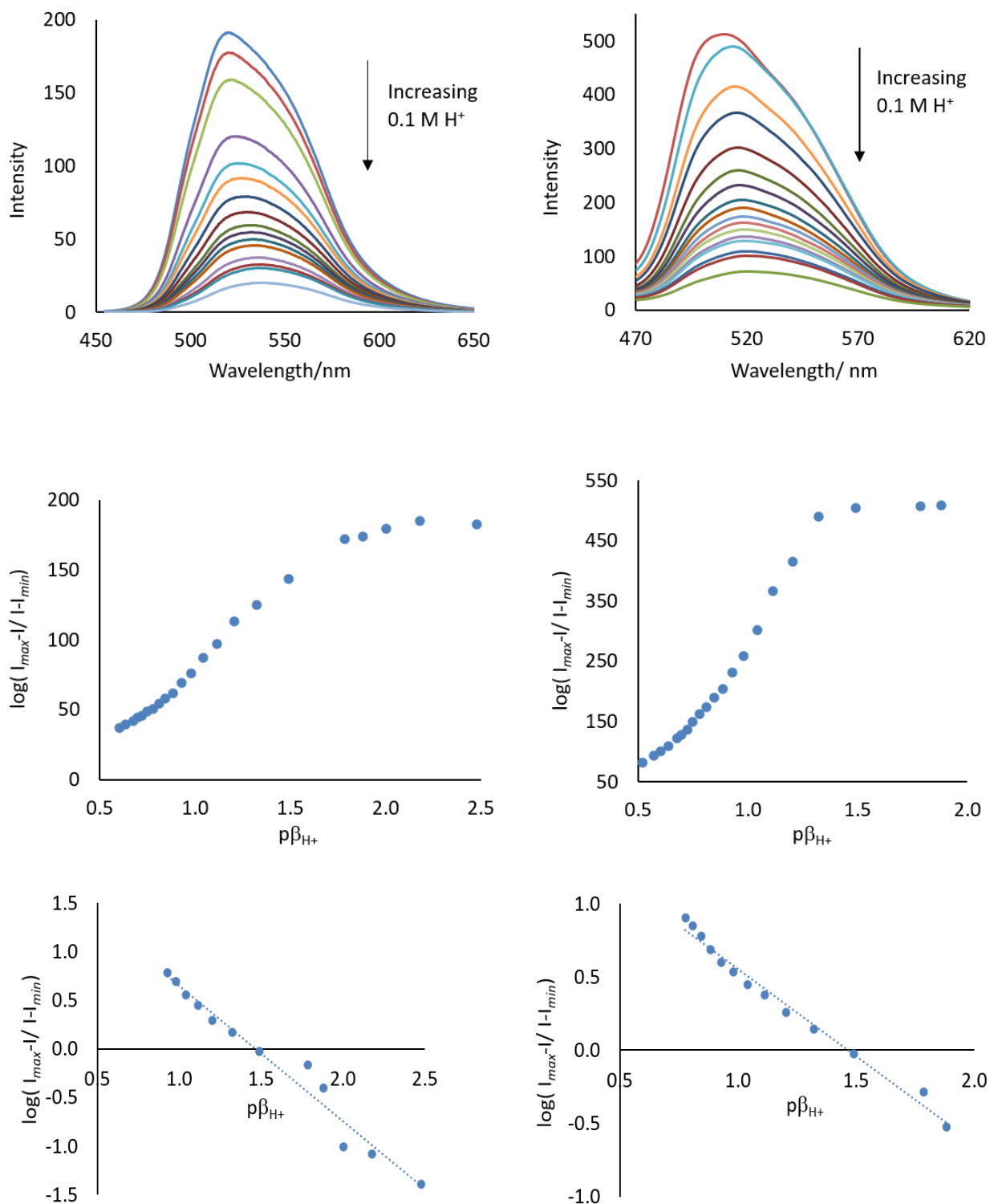


Fig.S20 Fluorescence spectra of 10 μ M **1** in THF titrated with 1 mM HCl solution excited at 440 nm (top). Titration curves from the peak intensity (middle). Linearized Henderson-Hasselbalch plots (bottom).

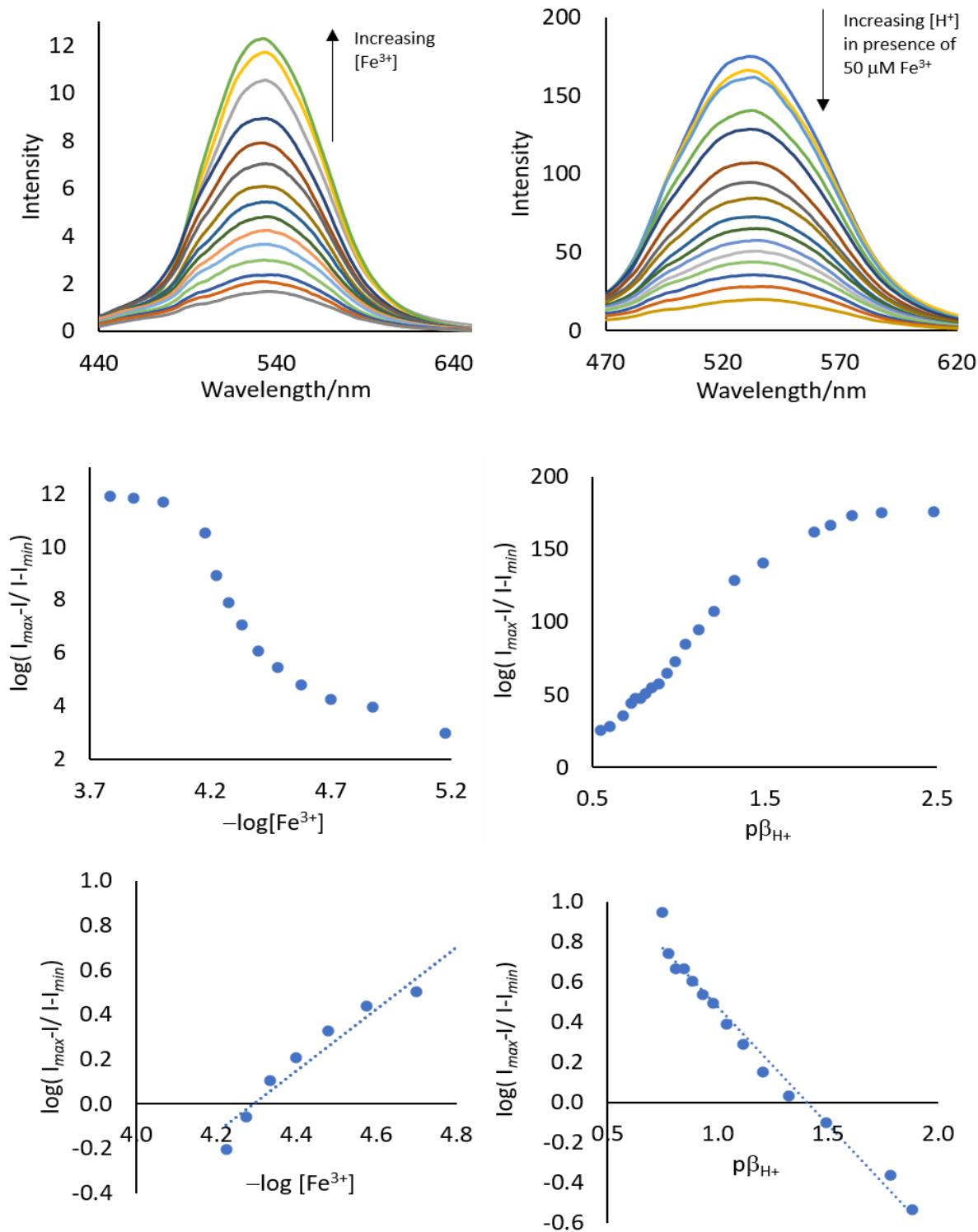


Fig.S21 Fluorescence spectra of 10 μM **3** in THF titrated with HCl solution and then with Fe³⁺ excited at 440 nm (top). Titration curves from the peak intensity (middle). Linearized Henderson-Hasselbalch plots (bottom).

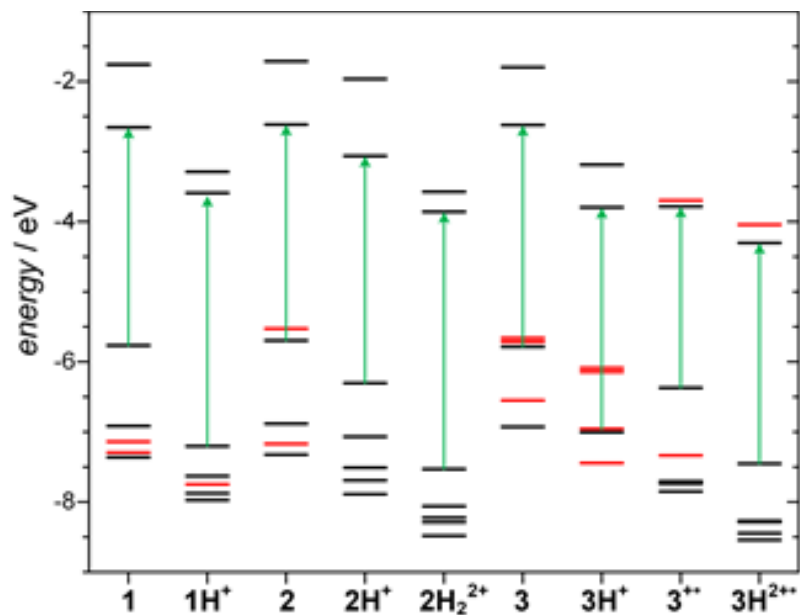


Fig. S22 Energy level HOMO-LUMO diagrams for **1–3** and their charged derivatives calculated at the B3LYP/6-31+g(d,p) level of theory with the IEFPCM solvent model for THF. Black lines indicate energy levels associated with the naphthalimide-pyrazoline framework, whereas the red lines with the 5-substituent (dimethylaniline or ferrocene). Green arrows indicate the lowest energy transition associated with the naphthalimide-pyrazoline chromophore. See Table S4 for energy level values.

Table S1. Summary of selected photophysical properties of **1** in various solvents.

| Solvent | Δf | λ_{abs} /nm | ν_{abs} /cm ⁻¹ | λ_{flu} /nm | ν_{flu} /cm ⁻¹ | $\Delta\lambda$ /nm | $\Delta\nu$ /cm ⁻¹ | ϵ | η | Φ_{F} |
|----------------------|------------|-------------------------------|---|-------------------------------|---|------------------------|----------------------------------|------------|--------|-------------------|
| Hexane | 0.000 | 430 | 232558 | 474 | 210970 | 44 | 21588 | 1.88 | 1.3749 | 0.36 |
| Benzene | 0.003 | 449 | 222717 | 498 | 200803 | 49 | 21914 | 2.28 | 1.5011 | 0.60 |
| Carbon tetrachloride | 0.011 | 451 | 221729 | 490 | 204082 | 49 | 17648 | 2.24 | 1.4600 | 0.61 |
| Chloroform | 0.149 | 459 | 217865 | 523 | 191205 | 64 | 26660 | 4.81 | 1.4458 | 0.20 |
| Diethyl ether | 0.167 | 444 | 225225 | 497 | 201207 | 53 | 24018 | 4.33 | 1.3530 | 0.47 |
| Ethyl acetate | 0.200 | 454 | 220264 | 520 | 192308 | 66 | 27957 | 6.08 | 1.3720 | 0.13 |
| Tetrahydrofuran | 0.210 | 457 | 218818 | 522 | 191571 | 65 | 27247 | 7.60 | 1.4072 | 0.08 |
| Pyridine | 0.212 | 466 | 214592 | 541 | 184843 | 75 | 29749 | 12.4 | 1.5093 | 0.06 |
| Dichloromethane | 0.219 | 459 | 217865 | 529 | 189036 | 70 | 28829 | 9.08 | 1.4241 | 0.09 |
| Octan-1-ol | 0.226 | 469 | 213220 | 540 | 185185 | 71 | 28034 | 10.3 | 1.4290 | 0.26 |
| Dimethylsulfoxide | 0.265 | 475 | 210526 | 550 | 181818 | 75 | 28708 | 48.9 | 1.4790 | 0.01 |
| Dimethylformamide | 0.275 | 468 | 213675 | 546 | 183150 | 78 | 30525 | 37.6 | 1.4305 | 0.01 |
| Acetone | 0.284 | 458 | 218341 | 539 | 185529 | 81 | 32812 | 20.7 | 1.3588 | 0.01 |
| Acetonitrile | 0.306 | 459 | 217865 | 537 | 186220 | 78 | 31645 | 38.8 | 1.3441 | 0.01 |
| Methanol | 0.309 | 470 | 212766 | 548 | 182482 | 78 | 30284 | 33.6 | 1.3284 | 0.00 |

Notations: orientation polarizability, Δf ; dielectric constant, ϵ ; refractive index, n ; absorption wavelength, λ_{abs} ; absorption wavenumber, $\nu_{\text{abs}} = 1/\lambda_{\text{abs}}$; emission wavelength, λ_{flu} ; emission wavenumber, $\nu_{\text{flu}} = 1/\lambda_{\text{flu}}$; Φ_{F} = fluorescence quantum yield.

Table S2. Summary of selected photophysical properties of **2** in various solvents.

| Solvent | Δf | λ_{abs} | ν_{abs} | λ_{flu} | ν_{flu} | $\Delta\lambda$ | $\Delta\nu$ | ϵ | η |
|----------------------|------------|------------------------|--------------------|------------------------|--------------------|-----------------|-------------------|------------|--------|
| | | /nm | /cm ⁻¹ | /nm | /cm ⁻¹ | /nm | /cm ⁻¹ | | |
| Hexane | 0.000 | 438 | 228311 | 482 | 207469 | 43 | 20842 | 1.88 | 1.3749 |
| Carbon tetrachloride | 0.011 | 440 | 227273 | 494 | 202429 | 54 | 24844 | 2.24 | 1.4600 |
| Diethyl ether | 0.167 | 450 | 222222 | 505 | 198020 | 55 | 24202 | 4.33 | 1.3530 |
| Benzene | 0.003 | 454 | 220264 | 511 | 195695 | 56 | 24570 | 2.28 | 1.5011 |
| Dichloromethane | 0.219 | 463 | 215983 | 540 | 185185 | 76 | 30798 | 9.08 | 1.4241 |
| Tetrahydrofuran | 0.210 | 454 | 220264 | 510 | 196078 | 56 | 24186 | 7.60 | 1.4072 |
| Chloroform | 0.149 | 470 | 212766 | 534 | 187266 | 64 | 25500 | 4.81 | 1.4458 |
| Acetone | 0.284 | 464 | 215517 | 541 | 184843 | 77 | 30674 | 20.7 | 1.3588 |
| Methanol | 0.309 | 474 | 210970 | 541 | 184843 | 67 | 26128 | 33.6 | 1.3284 |
| Pyridine | 0.212 | 464 | 215517 | 542 | 184502 | 78 | 31015 | 12.4 | 1.5093 |
| Dimethylformamide | 0.275 | 472 | 211864 | 547 | 182815 | 75 | 29049 | 37.6 | 1.4305 |
| Dimethylsulfoxide | 0.265 | 478 | 209205 | 554 | 180505 | 76 | 28700 | 48.9 | 1.4790 |

Notations: orientation polarizability, Δf ; dielectric constant, ϵ ; refractive index, n ; absorption wavelength, λ_{abs} ; absorption wavenumber, $\nu_{\text{abs}} = 1/\lambda_{\text{abs}}$; emission wavelength, λ_{flu} ; emission wavenumber, $\nu_{\text{flu}} = 1/\lambda_{\text{flu}}$;

Table S3. Frontier orbitals calculated for molecules **1–3** and their corresponding protonated and oxidized forms at the B3LYP/6-31+g(d,p) level of theory.

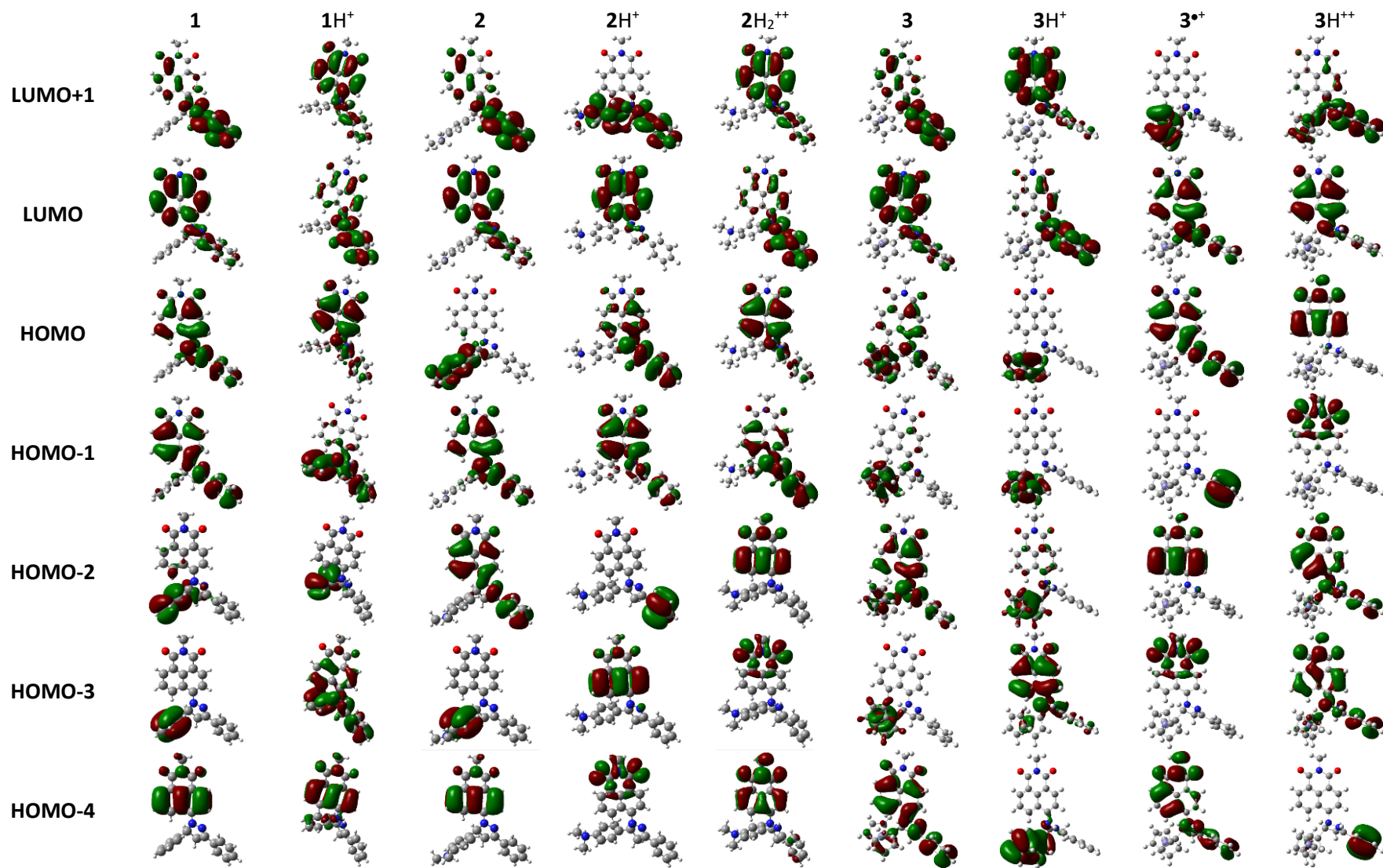


Table S4. Energies (in eV) of electronic levels of **1–3** and their charged derivatives as calculated at B3LYP/6-31+g level of theory with the IEFPCM solvent model for THF. The highest occupied and the lowest unoccupied orbitals for the naphthalimide-pyrazoline system (i.e. the levels engaged in the lowest energy electronic transition) are marked in blue, whereas orbitals associated with the substituent (quencher) are marked in red. $\Delta_{\text{HOMO-LUMO}}$ stands for the energy gap between the highest occupied and the lowest unoccupied orbitals of the chromophore.

| | 1 | 1H⁺ | 2 | 2H⁺ | 2H₂⁺⁺ | 3 | 3H⁺ | 3⁺ | 3H²⁺ |
|-----------------------------|----------|-----------------------|----------|-----------------------|------------------------------------|----------|-----------------------|----------------------|------------------------|
| LUMO+1 | -1.76 | -3.29 | -1.71 | -1.96 | -3.57 | -1.80 | -3.19 | -3.70 | -4.04 |
| LUMO | -2.65 | -3.59 | -2.61 | -3.06 | -3.86 | -2.62 | -3.80 | -3.78 | -4.30 |
| HOMO | -5.77 | -7.21 | -5.53 | -6.30 | -7.53 | -5.67 | -6.12 | -6.37 | -7.45 |
| HOMO-1 | -6.92 | -7.63 | -5.70 | -7.07 | -8.06 | -5.72 | -6.14 | -7.33 | -8.27 |
| HOMO-2 | -7.17 | -7.75 | -6.88 | -7.51 | -8.22 | -5.76 | -6.98 | -7.70 | -8.29 |
| HOMO-3 | -7.33 | -7.88 | -7.17 | -7.69 | -8.29 | -6.55 | -7.00 | -7.74 | -8.44 |
| HOMO-4 | -7.36 | -7.97 | -7.33 | -7.89 | -8.48 | -6.93 | -7.44 | -7.85 | -8.54 |
| $\Delta_{\text{HOMO-LUMO}}$ | 3.11 | 3.61 | 3.08 | 3.24 | 3.67 | 3.14 | 3.21 | 2.59 | 3.15 |